1 Methodology: Physics-Based Model

1.1 Problem Formulation

We develop a physics-based trajectory optimization framework for fuel-optimal cruise flight planning that explicitly models aircraft dynamics, fuel consumption, and meteorological wind effects. This model serves as a baseline for comparison against data-driven approaches.

The trajectory optimization is formulated as a nonlinear constrained optimization over a fixed-altitude cruise segment with multiple intermediate waypoints. The aircraft state evolves in continuous time while controls are discretized into K segments.

Decision Variables:

- Mach number profile: M_k for $k = 0, 1, \dots, K-1$
- Heading profile: ψ_k for $k = 0, 1, \dots, K-1$
- Waypoint passage times: $\tau_i \in [0, 1]$ for $i = 1, \dots, N_{\text{wp}}$
- Total flight duration: T (seconds)

Objective Function: The primary objective minimizes fuel burn with control smoothness regularization:

$$\min \quad J = m(0) - m(T) + \varepsilon \cdot R(M, \psi) \tag{1}$$

where $m(t)$ is aircraft mass at time t, and the regularization term is:

$$R(M, \psi) = \sum_{k=0}^{K-2} \left[(M_{k+1} - M_k)^2 + (\psi_{k+1} - \psi_k)^2 \right] \tag{2}$$

with $\varepsilon = 10^{-3}$ chosen to prevent oscillatory controls while remaining negligible relative to fuel burn.

Constraints:

1. *Terminal position*: $x(T) = x_f, \quad y(T) = y_f$. The aircraft must arrive precisely at the destination waypoint at the end of the flight segment.
2. *Waypoint passage*: $\|r(\tau_i \cdot T) - r_{\text{wp},i}\|^2 \leq R_{\text{wp}}^2$ for $i = 1, \dots, N_{\text{wp}}$. Each intermediate waypoint must be passed within a specified tolerance radius R_{wp}.
3. *Temporal ordering*: $\tau_i + \varepsilon_\tau \leq \tau_{i+1}$ where $\varepsilon_\tau = 10^{-3}$. Waypoints must be passed in the prescribed sequence.
4. *Operational bounds*: Mach number is bounded by aircraft-specific limits obtained from OpenAP performance data: $M_{\min} \leq M_k \leq M_{\max}$, where $M_{\max}$ is the maximum operating Mach number for the aircraft type. Heading angle is unconstrained: $-\pi \leq \psi_k \leq \pi$. Flight duration bounds are set based on route distance and expected speed range.

1.2 Aircraft Dynamics

1.2.1 Kinematic Model with Wind

The ground-track dynamics incorporate wind velocity following standard trajectory optimization formulations [2]:

$$\frac{dx}{dt} = V_{\text{TAS}} \cos(\psi) + w_u(x, y, t) \tag{3}$$

$$\frac{dy}{dt} = V_{\text{TAS}} \sin(\psi) + w_v(x, y, t) \tag{4}$$

where V_{TAS} is true airspeed (m/s), ψ is heading (rad), and w_u, w_v are eastward/northward wind components (m/s). Position (x, y) is expressed in local Cartesian coordinates via equirectangular projection.

True airspeed is computed from Mach number using ISA:

$$V_{\text{TAS}} = M \cdot a = M \cdot \sqrt{\gamma R T_{\text{ISA}}(h)} \tag{5}$$

where $\gamma = 1.4$, $R = 287.05$ J/(kg·K), and $T_{\text{ISA}}(h)$ is the ISA temperature at altitude h.

1.2.2 Fuel Flow Model

Fuel consumption is computed using the OpenAP framework [1], which provides validated fuel flow models for common aircraft types. For cruise flight at constant altitude:

$$\dot{m}_{\text{fuel}} = f_{\text{OpenAP}}(m, V_{\text{TAS}}, h, \text{VS} = 0) \tag{6}$$

where m is current mass, h is altitude, and VS = 0 enforces level flight. Mass evolves as:

$$\frac{dm}{dt} = -\dot{m}_{\text{fuel}}, \quad m(t) \geq m_{\text{min}} \tag{7}$$

1.3 Meteorological Wind Data

Wind fields are obtained from Japan Meteorological Agency (JMA) Global Spectral Model (GSM) Grid Point Value (GPV) forecasts in GRIB2 format [3]. We extract wind data at the 200 hPa or 250 hPa pressure level depending on the cruise altitude, which varies with seasonal tropopause height.

Data processing:

1. Load u, v wind components from GRIB2 using cfgrib/xarray
2. Spatially subset to Japan region (130°E–141°E, 33°N–36°N)
3. Convert to NumPy arrays for computational efficiency
4. Implement nearest-neighbor spatial interpolation for wind lookup

The wind field is treated as static over the short cruise duration ($\sim$15 minutes), which is appropriate for forecast sensitivity studies where we vary forecast initialization time rather than model temporal evolution.

1.4 Numerical Solution

The nonlinear program is solved using IPOPT (Interior Point OPTimizer) with automatic differentiation. Continuous-time dynamics are discretized using forward Euler with $K = 40$ steps, providing sufficient resolution while maintaining tractability.

At each time step k:

1. Compute V_{TAS} from Mach and altitude
2. Query wind field at current position
3. Update position: $x_{k+1} = x_k + \dot{x}_k \Delta t$, $y_{k+1} = y_k + \dot{y}_k \Delta t$
4. Update mass: $m_{k+1} = \max(m_k - \dot{m}_{\text{fuel},k} \Delta t, m_{\min})$

Solver settings: Convergence tolerance is set to 10^{-6}; iteration limits and CPU time bounds are adjusted as needed for problem scale.

Initialization: Mach number is initialized to the aircraft-specific typical cruise Mach from OpenAP. Heading is initialized along the great-circle direction: $\psi_k = \text{arctan}\,2(y_f - y_0, x_f - x_0)$. Waypoint passage times τ_i are linearly spaced, and flight duration is initialized to the midpoint of the feasible range.

2 Experimental Setup

Figure 1 shows the flight trajectories from the CARATS Open Data archive that traverse the study region. A total of 4,539 flights were identified passing through the YANKS–FLUTE corridor, providing the basis for selecting representative cases for optimization experiments.

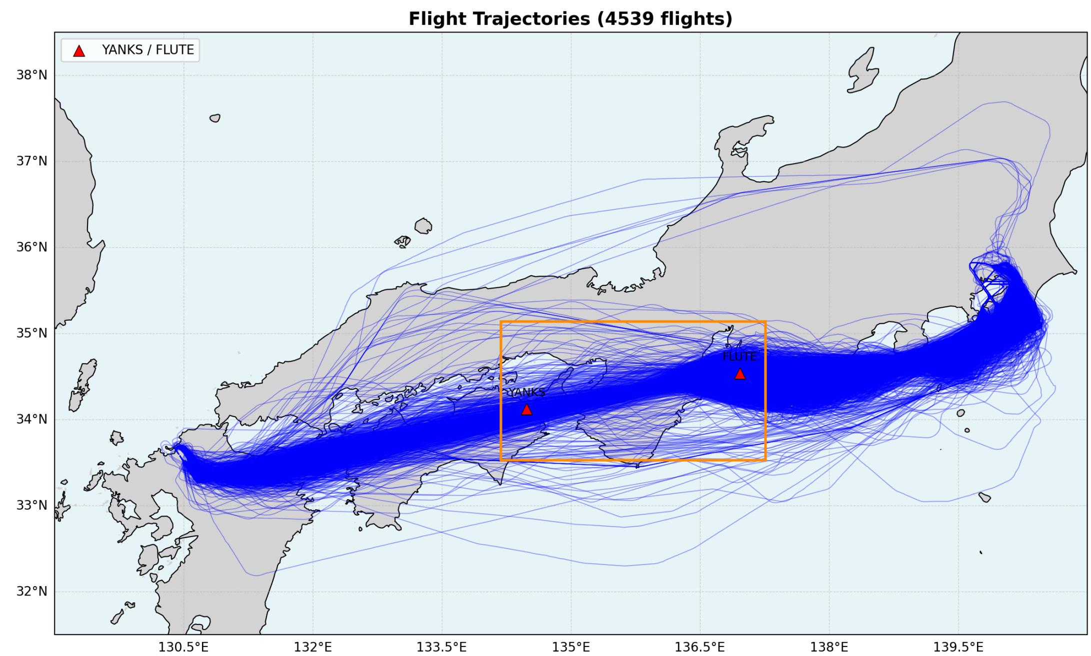

Figure 1: Flight trajectories from CARATS database (4,539 flights). The orange box indicates the YANKS–FLUTE study region.

2.1 Case Study: YANKS–FLUTE Route

We select a short-haul domestic route segment in Japan as our case study: YANKS $\rightarrow$ MIGEM $\rightarrow$ HALKA $\rightarrow$ LEKUT $\rightarrow$ FLUTE, approximately 125 NM in length. This segment represents the enroute cruise phase for flights operating between western Japan and the Tokyo metropolitan area.

This route was chosen for several reasons: (1) short-haul domestic flights in Japan are representative of high-frequency operations where fuel efficiency gains are operationally significant; (2) JMA GSM GPV forecast data provides high-quality wind coverage over this region; and (3) actual trajectory data from the CARATS Open Data archive is available for validation.

The altitude profile varies along the route as aircraft descend toward the terminal area. For optimization, we model fixed-altitude cruise segments at representative flight levels and analyze sensitivity to altitude selection.

2.2 Aircraft Configuration

Aircraft performance parameters are obtained from the OpenAP database, which supports multiple aircraft types. For each aircraft type, we extract the maximum operating Mach number ($M_{\max}$), typical cruise Mach, and fuel flow characteristics. Initial aircraft mass is set to 90% of maximum takeoff weight (MTOW). The waypoint tolerance radius is set to $R_{\mathrm{wp}} = 2000$ m, allowing minor deviations while ensuring waypoint compliance. Figure 2 shows the vertical profiles of flights traversing the study region across different seasons. Cruise altitudes typically range from FL350 to FL410, with seasonal variations reflecting tropopause height changes. Based on this analysis, we select FL330, FL390, and FL410 as representative cruise altitudes for optimization experiments, corresponding to 250 hPa and 200 hPa pressure levels for wind data extraction.

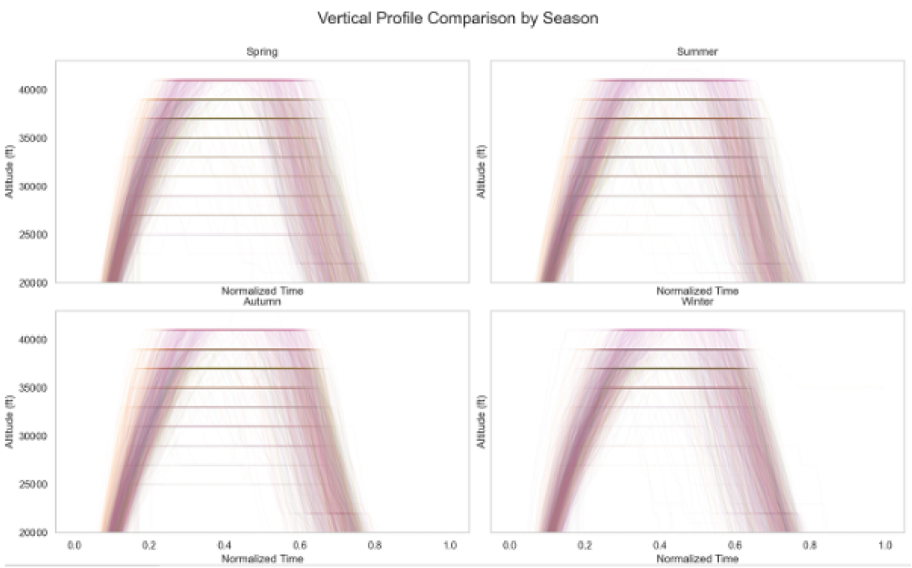

Figure 2: Vertical Profile

2.3 Forecast Lead Time Experiments

To investigate sensitivity to forecast lead time, we design experiments around actual flight departure times obtained from CARATS trajectory data. JMA GSM GPV forecasts are issued four times daily (00, 06, 12, 18 UTC) with forecast horizons extending to 120 hours at 6-hour intervals.

For a given flight departing at time t_{dep}, we select the most recent forecast initialization time $t_0 \leq t_{\text{dep}}$ as the baseline (near-zero lead time). We then progressively use earlier forecasts to simulate increasing lead times: 0, 6, 12, 18, 24, 30, 48, 72, 96, and 120 hours ahead of departure. This design reflects operational scenarios ranging from last-minute flight planning to strategic scheduling several days in advance.

Experiments were conducted for three representative dates spanning different seasons: February (winter), April (spring), and June (early summer). This seasonal variation captures differences in jet stream position and intensity, which significantly affect upper-level wind patterns over Japan.

2.4 Baseline Comparisons

Two baseline cases are established for comparison:

- *No-wind baseline*: Trajectory optimization without wind integration, isolating the effect of meteorological data on optimal solutions.
- *Time-optimal baseline*: Optimization minimizing flight duration rather than fuel burn, enabling analysis of the fuel–time tradeoff under different wind conditions.

Additionally, we compare results across multiple cruise altitudes to examine the interaction between altitude selection and wind-optimal routing. These comparisons also reveal limitations in the OpenAP fuel flow model at certain altitude and speed combinations.

3 Results

3.1 Effect of Wind Integration

To quantify the impact of wind modeling on trajectory optimization, we compare results with and without wind integration for the A320 at FL330 (April 2023 case). Table 1 summarizes the comparison.

Table 1: Comparison of optimization results with and without wind integration (A320, FL330)

Scenario	Duration (min)	Fuel Burned (kg)	Avg Tailwind (kt)
No wind	15.41	782.1	—
With wind (0h forecast)	13.31	675.5	40.2
Difference	−2.10 (−13.6%)	−106.6 (−13.6%)	—

The wind-integrated optimization yields a 2.1-minute reduction in flight time and 106.6 kg reduction in fuel burn compared to the no-wind case. This improvement is directly attributable to the $\sim$40 kt tailwind component along the route. The near-identical percentage reductions in duration and fuel (−13.6%) reflect the dominant role of ground speed in determining both metrics for cruise flight at constant altitude.

3.2 Forecast Lead Time Sensitivity

We conducted optimization experiments across five scenarios spanning different dates, aircraft types, and cruise altitudes. Table 2 summarizes the key results for each case.

Table 2: Summary of forecast lead time sensitivity across scenarios

Date	Aircraft / FL	Duration Range	Fuel Range	Tailwind Range
Apr 2023	A320 / FL330	29.4 sec	25.0 kg (3.7%)	33.6–44.4 kt
Apr 2023	A320 / FL390	19.8 sec	15.3 kg (2.5%)	49.4–56.9 kt
Apr 2023	A359 / FL410	18.0 sec	39.4 kg (2.4%)	49.4–56.9 kt
Jun 2023	A320 / FL330	25.2 sec	21.2 kg (3.1%)	33.9–42.2 kt
Feb 2024	FL410	11.4 sec	16.9 kg (1.7%)	69.5–75.2 kt

Across all scenarios, the variation in optimized flight duration due to forecast lead time remains within approximately 30 seconds. This limited sensitivity can be attributed to several physical factors: (1) the short route distance (∼125 NM) limits the cumulative effect of wind prediction errors; (2) the ratio of wind speed variation to true airspeed is small (typically 4–5%); and (3) the large ground speed baseline (∼450 kt) dampens the relative impact of wind uncertainty.

Figure 3 shows the detailed forecast sensitivity for the April 2023 A320 FL330 case, which exhibits the largest variability among all scenarios. Figure 4 shows the February 2024 FL410 case, demonstrating the most stable predictions due to strong winter jet stream conditions.

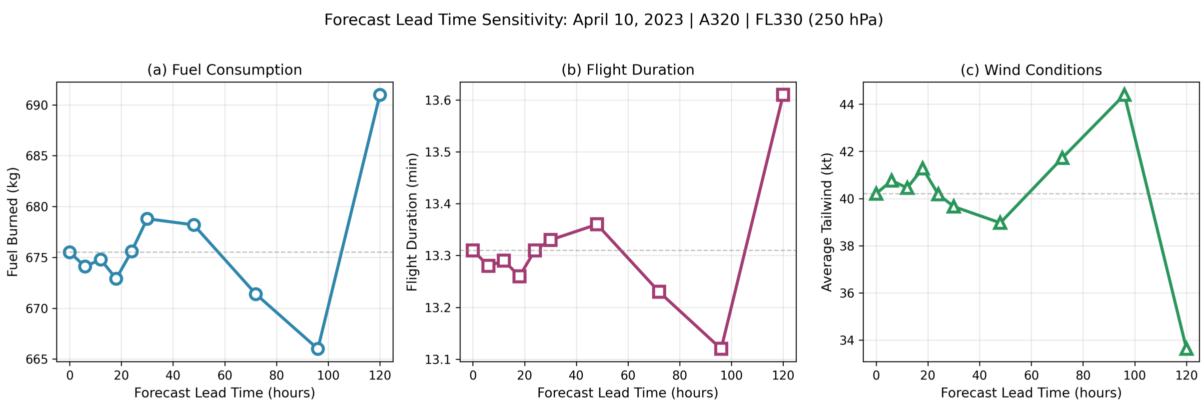

Figure 3: Forecast lead time sensitivity for April 2023, A320 at FL330 (250 hPa). This case shows the largest variability among tested scenarios.

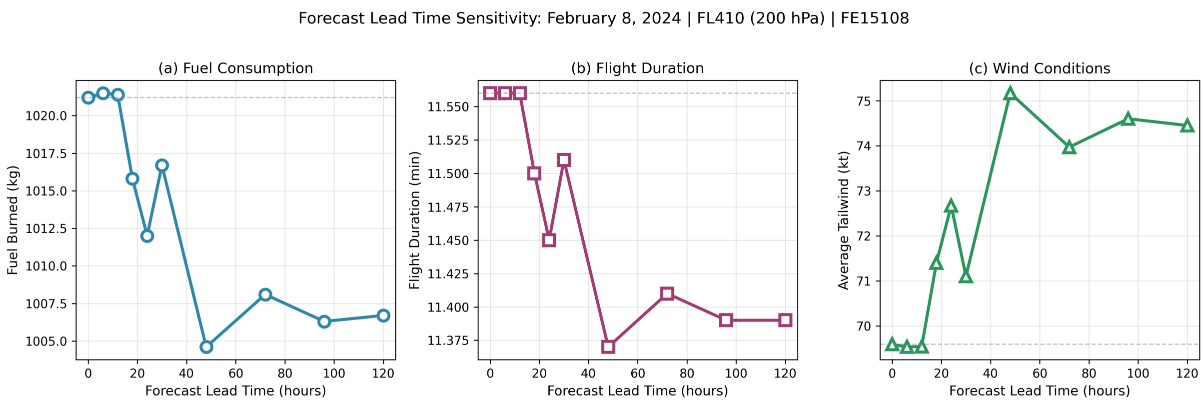

Figure 4: Forecast lead time sensitivity for February 2024, FL410 (200 hPa). Strong winter jet stream results in highly stable predictions across all lead times.

Figure 5 shows the flight duration deviation from the 0-hour baseline across all scenarios. The February case exhibits the smallest deviation (within ±10 seconds), attributable to the stable and strong winter jet stream conditions, with consistent tailwinds exceeding 70 kt. In contrast, the April and June cases at FL330 show larger variability, reflecting weaker and less predictable wind patterns at lower altitudes.

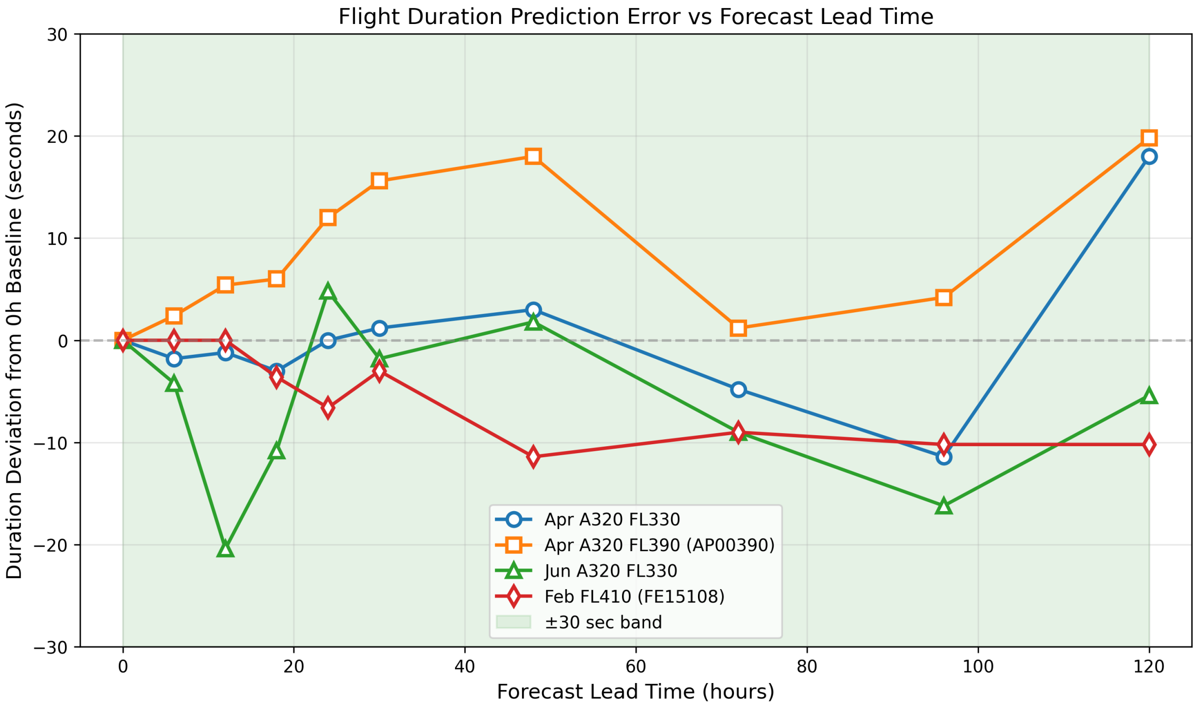

Figure 5: Flight duration deviation from 0-hour baseline forecast across all scenarios.

3.3 Comparison with Actual Flight Data

For three scenarios, actual flight times from CARATS trajectory data are available for validation. Table 3 compares predicted and actual flight durations.

Table 3: Comparison of predicted vs. actual flight duration

Flight ID	Aircraft / FL	Actual (min)	Predicted 0h (min)	Error
AP00390	A320 / FL390	15.81	12.73	−3.08 min (−19.5%)
AP00393	A359 / FL410	14.61	12.14	−2.47 min (−16.9%)
FE15108	FL410	11.37	11.56	+0.19 min (+1.7%)

The results reveal two distinct patterns. The February flight (FE15108) shows excellent agreement between predicted and actual duration, with an error of only 11 seconds (1.7%). Notably, the 48-hour forecast prediction (11.37 min) matches the actual flight time exactly. This suggests that for stable winter jet stream conditions, the physics-based model provides highly accurate predictions even with extended forecast lead times.

In contrast, the April flights (AP00390, AP00393) show systematic under-prediction of flight time by 2–3 minutes (17–20%). This discrepancy likely reflects factors not captured in the optimization model:

- Air traffic control constraints requiring non-optimal speed or heading adjustments

- Actual flight paths deviating from the idealized waypoint sequence
- Conservative speed schedules adopted by operators for fuel contingency
- Descent or climb segments within the study corridor not modeled in cruise-only optimization

These findings highlight both the potential and limitations of physics-based trajectory prediction: under favorable conditions (stable winds, unconstrained airspace), the model achieves high accuracy; under operationally constrained conditions, systematic biases emerge that data-driven methods may better capture.

3.4 Altitude and Seasonal Effects

The results reveal a clear relationship between cruise altitude and forecast sensitivity. Higher flight levels (FL390, FL410) experience stronger and more consistent upper-level winds, resulting in:

- Shorter flight durations (11–13 min vs. 13–14 min at FL330)
- Lower fuel burn sensitivity to forecast lead time (1.7–2.5% vs. 3.1–3.7%)
- More stable tailwind conditions across different forecast horizons

Seasonal effects are also evident. The February 2024 case demonstrates remarkably stable predictions across all lead times, with duration varying by only 11.4 seconds over the 0–120 hour forecast range. This stability reflects the strong, persistent jet stream characteristic of winter months over Japan. The June case shows more erratic behavior, with the 12-hour forecast yielding lower fuel burn than the 0-hour baseline—indicating that forecast "errors" do not monotonically increase with lead time but depend on synoptic weather evolution.

3.5 Wind Field Visualization

Figure 6 illustrates the 250 hPa wind speed field for different forecast lead times. The wind speed difference plots (relative to FD0000) reveal that forecast errors are not uniformly distributed spatially. Along the YANKS–FLUTE route corridor, forecast deviations of ± 5–10 m/s are typical for lead times beyond 48 hours. These localized wind prediction errors directly translate to the fuel and duration variability observed in the optimization results.

3.6 Implications for Flight Planning

The results suggest that for short-haul routes similar to the YANKS–FLUTE segment, physics-based trajectory optimization using wind forecasts up to 48–72 hours ahead yields flight time predictions within approximately 20–30 seconds of near-real-time optimization. This finding has practical implications:

1. *Strategic planning*: Fuel load calculations based on 2–3 day forecasts introduce only marginal uncertainty ($<3\%$ fuel variation) for short domestic segments.
2. *Slot allocation*: Predicted waypoint passage times remain reliable within ± 30 seconds even with day-ahead forecasts, supporting air traffic flow management.
3. *Model limitations*: The deterministic physics-based approach provides a single optimal trajectory for each forecast scenario but cannot directly quantify prediction confidence intervals—a limitation that data-driven or ensemble methods may address.

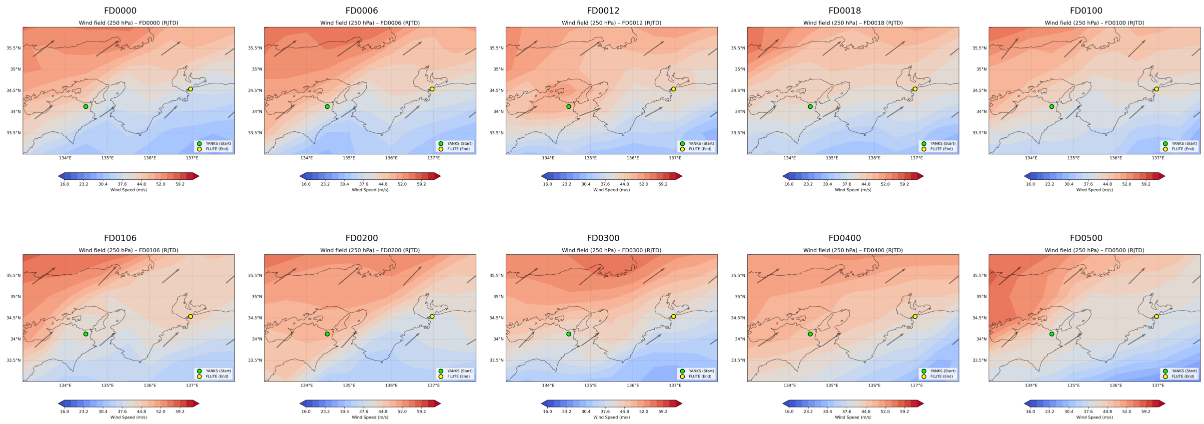

Figure 6: Wind speed field (m/s) at 250 hPa for various forecast lead times. YANKS (start) and FLUTE (end) waypoints are marked.

References

[1] Sun, J., Hoekstra, J. M., and Ellerbroek, J.: OpenAP: An open-source aircraft performance model for air transportation studies and simulations, *Aerospace*, Vol. 7, No. 8 (2020), p. 104.

[2] Sun, J.: OpenAP.top: Open flight trajectory optimization for air transport and sustainability research, *Aerospace*, Vol. 9, No. 7 (2022), p. 383.

[3] Japan Meteorological Agency: Global Spectral Model (GSM) Grid Point Value Data, Kyoto University RISH Archive, https://database.rish.kyoto-u.ac.jp/arch/jmadata/data/gpv/original/ (accessed 2024).